LARGE EDDY SIMULATION OF OBLIQUE FLOW PAST A CUBICLE OBSTACLE

Demetri G. Bouris
Department of Engineering and Management of Energy Resources
University of Western Macedonia
Kastorias & Fleming 1, 50100, Kozani, Greece
dmpouris@uowm.gr

Andreas P. Theodorakakos
Fluid Research Co.
Laskareos 49, 11472, Athens, Greece
fluidresearch@in.gr

George C. Bergeles
Department of Mechanical Engineering
National Technical University of Athens
Her. Polytechniou 9, 15700, Zografou, Greece
bergeles@fluid.mech.ntua.gr

ABSTRACT
Oblique flow past a cube or low rise structure is of importance in designing and constructing structures and buildings, among other applications. In the present study the large eddy simulation (LES) methodology is applied on an unstructured grid with locally refined resolution in order to study the surface pressure field and the conical vortices that develop on the roof of a low rise cubicle. Three simulations are performed, evaluating the effect of temporal and spatial resolution and results are compared to experimental measurements and to a point vortex theory for the conical vortex structure. Spatial resolution is found to be of importance in correct representation of the conical vortex structure as well as the high frequency spectrum of the roof-top pressure fluctuations.

INTRODUCTION
The goal of achieving wind resistant structures and buildings continues to play an important role during the design and construction phase, especially in areas that are susceptible to high wind velocities or instantaneous gusts of winds. An especially complex condition arises when a cube shaped obstacle or low-rise structure with a square roof is placed under an oblique incident flow as strong conical vortices are formed on the leading edges of the roof. Experimental studies (Kawai and Nishimura, 1996, Marwood and Wood, 1997) have proven that their behavior is of a complex fluctuating nature and that large values of instantaneous negative pressures appear. The advantage of accurate numerical simulations of this condition is obvious but it has proven to be quite difficult since most studies published using steady state calculations with the k-ε turbulence model fail to reproduce even the conical vortices. Specifically tuned modifications to the standard k-ε model such as the Murakami-Mochida-Kondo (MMK) model (Tsuchiya et al., 1997) have also appeared, providing some improvement but still unable to reproduce characteristics of the unsteady flow. Relatively recently, large eddy simulations of the flow in question have also begun to appear in the literature, although with a high calculation cost and unresolved issues related to discretisation, subgrid scale modelling and Reynolds number independance. Thomas and Williams, (1999) presented LES calculations of the 45° skewed flow past a surface mounted cube. They used multi-grid domain decomposition and MPI parallel programming in order to attain reasonable computing times with 32 grid cells on the cube sides and a total of $8 \cdot 10^6$ nodes in the computational domain. Two LES calculations of the same oblique flow past a cubicle, whose height was half that of the other two dimensions, have also been presented (Tamura et al. 1997). The two simulations differed in Reynolds number, convection term discretisation scheme and subgrid scale model and their results were so different that the effect of the subgrid scale model and the convection term discretisation was further investigated, although not for the case of the oblique flow. Furthermore, although the calculations and experiment to which they were compared were at different flow Reynolds numbers, the matter of Reynolds number independence remained unresolved. In the present study, the oblique, 45°, flow past a cubicle obstacle is calculated using a large eddy simulation. An unstructured grid is used in order to minimise computational effort while still achieving sufficient detail in the simulation. Parameters such as the temporal and spatial discretisation are investigated through variation of the time step and local refinement of the grid in the regions of the conical vortices' development. Results are compared with available experimental measurements of pressure coefficient distribution and fluctuation on the surfaces of the obstacle.

NUMERICAL METHODOLOGY
The governing Navier - Stokes conservation equations of the flow field are numerically solved on an unstructured grid, following the finite volume approximation and a pressure correction method. The time dependent mass and momentum equations are expressed for an arbitrary coordinate system and

for cartesian velocity components. The mass conservation equation is:

$$\frac{\partial \rho}{\partial t} + \nabla \cdot \rho \vec{u} = 0 \tag{1}$$

where (ρ) is density, (t) time and ($\vec{u}$) the velocity vector. The momentum conservation equation is

$$\begin{aligned} &\frac{\partial \rho \vec{u}}{\partial t} + \nabla \cdot \left(\rho \vec{u} \otimes \vec{u} - \overline{T} \right) = \vec{S}_u \\ &\overline{T} = -\left(P + \frac{2}{3} \mu_{eff} \nabla \cdot \vec{u} \right) \overline{I} + \mu_{eff} \left(\nabla \otimes \vec{u} + (\nabla \otimes \vec{u})^T \right) \end{aligned} \tag{2}$$

where $\otimes$ is the vector product, ($\overline{T}$) is the stress tensor, (P) the pressure, (μ_{eff}) the effective viscosity of the fluid, ($\overline{I}$) is the unit tensor and ($\vec{S}_u$) represents the added source terms. The effective viscosity is defined according to the Smagorinsky model (Smagorinsky, 1963):

$$\begin{aligned} &\mu_{eff} = \mu + \mu_t \\ &\mu_t = \rho (C_s \Delta)^2 \sqrt{\overline{S} \cdot \overline{S}}, \quad \overline{S} = \nabla \otimes \vec{u} + (\nabla \otimes \vec{u})^T \end{aligned} \tag{3}$$

where (μ) is the fluid dynamic viscosity, (S_{ij}) is the strain rate, (Δ) is a length scale, taken here as the cubic root of the cell volume and (C_s) a constant equal to 0.1.

The transport equations are integrated and discretised over the common control volume following the finite volume method. The grid that is used for the present case is an unstructured mesh, where every cell has an arbitrary number of faces and neighboring cells. In this way, no special treatment is needed when applying local refinement to a region. The grid arrangement is collocated, where all the unknown variables are stored in the center of the computational cell. In order to avoid pressure - velocity decoupling problems, arising from the fact that pressure and velocities are calculated in the same location, the convective flux through each cell face is calculated using a modification based on that of Rhie and Chow (1983). The key feature of this approach is that the velocity used to calculate the convective flux through a cell face, is not calculated by a linear interpolation of the adjacent cells velocities, but is modified to be directly linked to the two adjacent pressure nodes. Following this procedure, a pressure prediction - correction method (resembling the well known SIMPLE algorithm of Patankar and Spalding, 1972) is used in order to derive the pressure equation from the continuity equation. In the present study, in order to avoid problems related to numerical damping often associated with upwind schemes, all terms are discretised using the standard second order central difference scheme. For temporal discretisation, the second order semi-implicit Crank Nicholson scheme is used. The set of the linear equations that result after the discretisation of the conservation equations, are solved based on an LU decomposition, although in some cases switching to a GMRES solver provided better stability.

RESULTS

In the present study a large eddy simulation of oblique (45°) turbulent flow past a half-height cubicle obstacle (dimensions: 0.2x0.1x0.2 m) is performed on a fully unstructured computational mesh. The Reynolds number of the flow is 6450, based on the uniform upstream velocity (U_o) and the side of the roof (2h) (h is the height of the obstacle), a value also used in the calculations presented in Tamura et al. (1997). Although the experimental measurements' Reynolds number was an order of magnitude higher, it is assumed that the main characteristics of the flow, with the exception of the peak negative pressure coefficients on the roof, will retain similarity. Similarity of the rooftop pressure distributions is also mentioned in the original work of Castro and Robins (1977) for turbulent flow past a cube.

Extra care was taken to construct the grid so that both the no-slip condition could be implemented and the wall function assumption avoided while keeping the number of grid points relatively low. The use of the unstructured mesh helps in this direction aided by the use of a locally refined grid at specific regions of the flow, as will be described later in the paper. For use of the no-slip condition, the largest distance of the nearest grid point to the obstacle was h/100, giving a mean $y^+<2$ on the roof. The initial grid consisted of 380,000 hexahedral cells with 40 cells defining the side of the obstacle. The grid defined length scale (Δ) near the surface of the obstacle is slightly below the value of the Taylor length scale, estimated from $\lambda=h\cdot(15/Re_h)^{0.5}$ (Tennekes and Lumley, 1974). This provides a sufficient spatial resolution, as verified by the SGS viscosity values, which were found not to exceed a value of 3-4 times that of the fluid dynamic viscosity.

The effect of grid size was evaluated in a calculation with a locally refined region where the conical vortices develop i.e. from the upstream corner to the rear edges. The discretisation in this region was doubled in each direction by dividing each cell in that region into 8 smaller ones, resulting in a total grid size of 480,000 hexahedral cells. Close ups of the region near the cubicle for both the grids that were used are shown in Figure 1. It has been mentioned in the literature (Murakami, 1998) that grid non-uniformity could cause numerical oscillations since the cut off wave number (Δ), which is dependent on grid size, changes abruptly. This might be the reason that attempts to perform the calculations at a higher Reynolds number lead to severe instabilities in the numerical procedure. In the present calculations, no oscillations were detected, at least not in the wall adjacent regions where results are presented.

Two time steps were also used for the calculations i.e. dt=5.E-4 sec and dt=5.E-3 sec. For the larger of the two time steps and the locally refined grid, the maximum CFL number was 1.4 and the computational cost was 6.5 time steps/hour on a 2.6 GHz P4 personal computer using ~500 MB of RAM.

The present study aims to take advantage of the unstructured grid in order to resolve small scale structures near the obstacle and to numerically reproduce the characteristics of the conical

vortices' development that have been experimentally observed.

As an initial condition, a steady state k-ε simulation was performed. From this steady state solution, the large eddy simulation studies began with a steady, uniform incoming flow, slip conditions (i.e. zero 1st gradient) for the top and side boundaries and constant 1st gradient in the flow direction for the outlet. The boundary conditions were considered acceptable considering the distance of the computational domain boundaries from the obstacle: 7.5h and 12.5h upstream and downstream respectively and 10h above and on either side of the obstacle. Three different simulations were performed: one with the grid resolution shown in Figure 1b and a time step of dt=5E-3s, another with the same grid resolution and a time step of dt=5E-4s and a third with the locally refined grid shown in Figure 1a and a time step of dt=5E-3s. The three simulations will be compared to the experimental measurements and the respective steady state calculations using the MMK model presented in Tsuchiya et al., (1997) and to the experimental measurements of Kawai & Nishimura (1996). It should be mentioned that for all LES calculations, mean values were calculated by averaging flow results for at least 25 large eddy turnover times (h/U_o). Longer calculation times would mainly lead to improvement in the resolution of turbulence statistics and very low frequencies. Computational cost was the basic parameter preventing further calculation and insight into low frequency fluctuations but the present level of resolution was considered adequate for evaluating the effect of time step and grid resolution as well as acquiring information regarding the characteristics of the conical vortices.

Snapshots of the calculated vortex development and shedding are portrayed in Figure 2 using iso-pressure surfaces based on the pressure coefficient $C_p = (P - P_o)/(0.5\rho U_o^2)$ with (P_o) the upstream static pressure at the inlet and at the cubicle height. It is interesting to note how the conical vortex from the leading edge of the right hand side (negative x direction) of the roof of the cubicle develops downstream where it interacts and is trapped by the recirculation zone of the vertical side edge.

As an indication of the highly varying pressure values arising from the unsteady nature of the conical vortices on the roof of the obstacle, the instantaneous distribution of the pressure coefficient, at a distance of one cube height from the leading corner and in a direction perpendicular to the flow, has been plotted in Figure 3 for a number of time steps corresponding to a total of 10 large eddy turnover times ($10h/U_o$). The results are from the calculation without local grid refinement and with a time step of 5E-3s. The highly varying peak values of the pressure coefficient are obvious and their position on the roof is relatively constant in time indicating that the swaying motion has not been reproduced. Simulation of the vortex swaying observed by Kawai (2002) would require very long calculation times and the present study was not extended in this direction. However, as will be shown following, the high frequency fluctuation seems to have been well represented.

Regarding the structure of the vortices, results are presented in Figure 4 comparing with experimental measurements and a point vortex theory according to Kawai and Nishimura (1996). Assuming a non-viscous point vortex at a distance of z_{max} from the top surface of the cubicle and with the vortex axis parallel to the cubicle's roof, the pressure distribution can be calculated as:

$$\frac{\Delta C_P}{\Delta C_{P_{max}}} = \left[(\delta/z_{max})^2 + 1\right]^{-2}, \quad z_{max} = b/\sqrt{\sqrt{2}-1} \qquad (4)$$

Eq. (4) requires an alternative coordinate system on the roof plane, as indicated in the illustrative figure in Figure 4, where (δ) is the direction perpendicular to the side of the roof (s) and δ=0 at $\Delta C_{p,max}$. (b) is the half width i.e. the distance in the (δ) direction where the pressure profile reaches half the maximum value. If the mean pressure coefficient distributions in the direction perpendicular to the side of the roof (δ) are expressed in this coordinate system, then a similarity law is found to exist. The results for the three different calculations are presented in Figure 4. For all three calculations, the profile of the mean pressure coefficient is very close to the experimental measurements and the point vortex theory in the downstream positions, where the vortices have already developed significantly. In the region close to the leading corner of the cubicle, the two calculations without the local grid refinement (Figure 4a and b) exhibit a discrepancy in relation to the measurements and the theory. Judging from the results of the case with local grid refinement (Figure 4c) it can safely be stated that this is a result of limited spatial resolution in a region of significant flow development and instability. Refining the grid leads to a remarkable agreement with theory and experiments. It should be reiterated here that the flow Reynolds number in the calculations is an order of magnitude lower than in the experiments and yet the similarity law describing the structure of the vortices still holds, even compared to a non-viscous point vortex theory.

More detailed comparison is shown in Figure 5 - Figure 7 where calculated mean pressure coefficients are plotted for all three presently performed LES calculations, the experimental measurements presented in Tsuchiya et al. (1997) and the calculations using the MMK model also presented in Tsuchiya et al. (1997). The MMK model is a k-ε modification which aims at reducing the excessive production of turbulence kinetic energy by introducing a modified expression for the production term as a function of strain rate and local vorticity. The differences between the three LES calculations are not very pronounced although one would have expected it considering the improvement brought on by the grid refinement in the pressure profile similarity calculations (Figure 4). Furthermore, the peak pressure value is underestimated in the distribution on the top of the roof (Figure 7). One possible explanation for this might be that the Reynolds number of the experimental measurements is almost an order of magnitude higher than that of the simulations. Although the similarity law is correctly reproduced, the absolute peak value might be more strongly related to the upstream flow Reynolds number. Another important point that should be made is the fact that all three LES calculations correctly reproduce a local maximum of the peak negative pressure coefficient at a distance from the edge of the roof instead of at the edge as does the MMK model, for example. However, the MMK model did exhibit the correct behavior for smaller angles of attack (0^o, 22.5^o).

Further insight into the structure of the conical vortices can be gained from Figure 8 which portrays the calculated mean flow field, for the calculation with the locally refined grid, on a plane

normal to the main flow direction (xy) passing through the center of the cubicle (z=0). The vortex cores are clearly discernible from the position where the transverse velocity changes sign. Their elevation from the roof has been calculated from a number of similar planes perpendicular to the flow (not shown for lack of space) as being constant along the roof and at 16% of the cube height. For a 45° angle of attack, Marwood and Wood (1997) measured an elevation of 11% the cube height. From the point of peak negative pressure for the profiles presented in Figure 4c the angle of the vortex axis relative to the side of the roof can also be calculated. This was found to be 10.5° as compared to 12.8° measured by Kawai and Nishimura (1997). A possible reason for the discrepancy in both the calculated elevation and the angle of the conical vortices is that the Reynolds number of the experimental measurements is an order of magnitude higher with the flow possibly pushing the vortices inwards from the edge and down towards the roof.

Looking into the level of resolution in the high frequency part of the pressure coefficient fluctuation, we arrive at Figure 9. Here the fluctuation of the pressure coefficient is taken from the LES simulation by subtracting the local mean value from the instantaneous one and then the power spectral density is calculated in non dimensional form and plotted against non-dimensional frequency:

$$\mathrm{PSD} = \frac{f \cdot S(f)}{0.5\rho U_o^2}, \quad \mathrm{St} = \frac{f \cdot 2h}{U_o} \tag{5}$$

where S(f) is the absolute value of the Fourier transform of the time series. The experimentally obtained spectrum by Kawai and Nishimura (1996) is also plotted in Figure 9 for comparison. Figure 9a shows results for the calculation using dt=5E-3s and the grid without local refinement. The energy levels seem to be correct but the slope in the high frequency range is not the same as the (-5/3) slope measured in the experiments and indicated by a straight line in the figure. The lower frequency portion of the spectrum has not been reproduced since it is a function of total calculation time, as is the resolution in the frequency spectrum. Reducing the minimum resolved frequency by half would require doubling the total number of time steps calculated. With the locally refined grid and the same time step (Figure 9b), the slope in the high frequency range is closer to that measured in the experiments, indicating a better resolution not only of the energy level in the high frequency fluctuation of the roof-top pressures but also the correct energy distribution. The energy level in the low frequency part of the spectrum seems to be at the correct level, although a better resolution is desirable in this region. Besides the matter of the long computational time, it is important to mention that an attempt to explain the low frequency swaying of the vortices has led to the quasi steady theory (Marwood and Wood, 1997). According to this, the swaying is a result of the variation in attack angle due to upstream turbulence (see also Kawai, 2002) and the vortices respond to this as if all of the mean upstream flow had changed direction. In a simulation with a steady, uniform upstream flow, this may be the reason that vortex swaying was not observed. An interesting numerical experiment would be to introduce an upstream fluctuating field in order to determine its effect on the vortex behaviour.

If the observations concerning the frequency range are combined with those mentioned previously for the mean pressure coefficients, then one could justify the improved reproduction of the conical vortex similarity law by the correct reproduction of the high frequency spectrum. However, it is important to note that in LES this requires both adequate temporal and spatial resolution and it is to this effect that unstructured grids, local grid refinement techniques, or both, can be effectively used.

CONCLUSIONS

Large eddy simulation of the flow at a 45° angle of attack to a cubicle obstacle of dimensions (2h, h, 2h) is performed on a fully unstructured mesh. The temporal and spatial resolution have been evaluated by employing two time steps, an order of magnitude apart, and a locally refined grid in the regions where the conical vortices develop. Results indicate that the effect of the locally refined grid is significant in the correct reproduction of the form of the conical vortices through comparison with an experimentally confirmed similarity law. This could be attributed to the improved resolution of the high frequency spectrum, as observed by prediction of the power density spectrum.

With regard to numerical matters, it is reiterated that the importance of spatial resolution, especially in LES, cannot be underestimated. On the other hand, in terms of understanding the mechanism behind conical vortex behaviour it might be warranted to look further into the effect of the high frequency spectrum, a matter that is sometimes overlooked in relation to upstream conditions of the flow (e.g. mean onset angles, quasi-steady theory etc.).

REFERENCES

Castro I. and Robins A., 1977, "The flow around a surface mounted cube in uniform an turbulent streams". *J. Fluid Mech.*, Vol. 79, No. 2, pp. 307-335.

Kawai H, Nishimura G., 1996, "Characteristics of fluctuating suction and conical vortices on a flat roof in oblique flow". *J. Wind Eng. Ind. Aerodyn.* Vol 60, pp. 211-225.

Kawai H., 2002, "Local peak pressure and conical vortex on building." *J. Wind Eng. Ind. Aerodyn.*, Vol 90, pp. 251-263.

Marwood R. and Wood C.J., 1997, "Conical vortex movement and its effect on roof pressures" *J. Wind Eng. Ind. Aerodyn.*, Vol. 69-71, pp. 589-595.

Murakami S., 1998, "Overview of turbulence models applied in CWE-1997", *J. Wind Eng. Ind. Aerodyn.*, Vol.74-76, pp.1-24.

Patankar SV, Spalding BD., 1972, "A calculation procedure for heat, mass and momentum transfer in three-dimensional parabolic flows" *Int. J. Heat and Mass Transfer,* Vol. 15, pp. 1787-1806.

Rhie MC, Chow LW., 1982, "A Numerical Study of the Turbulent Flow Past an Isolated Airfoil with Trailing Edge Separation." AIAA-82-0998.

Smagorinsky J., 1963, "General circulation experiments with the primitive equations, (i) the basic experiment". *Monthly Weather Rev*, Vol. 91(3), pp.99–164.

Tamura T., Kawai H., Kawamoto S., Nozawa K., Sakamoto S. and Ohkuma T, 1997, "Numerical prediction of wind loading on buildings and structures – Activities of AIJ cooperative project on CFD." *J. Wind Eng. Ind. Aerodyn.* Vol. 67&68, pp. 671-685.

Tennekes H. and Lumley J.L., 1974, "A first course in turbulence", MIT Press.

Thomas T.G. and Williams J.J.R., 1999, "Simulation of skewed turbulent flow past a surface mounted cube." *J. Wind Eng. Ind. Aerodyn.* Vol 81, pp. 347-360.

Tsuchiya M., Murakami S., Mochida A., Kondo K. and Ishida Y., 1997, "Development of a new k-ε model for flow and pressure fields around bluff body" *J. Wind Eng. Ind. Aerodyn.* Vol. 67&68, pp. 169-182.

FIGURES

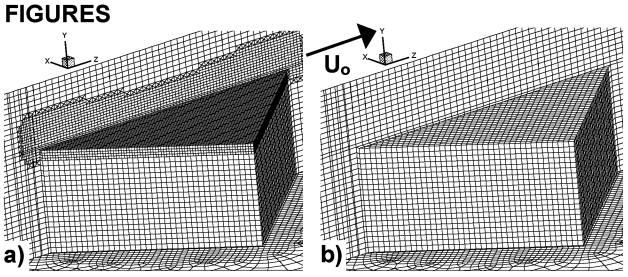

Figure 1. Unstructured meshes used in the simulation a) locally refined with 480,000 cells and b) 380,000 cells.

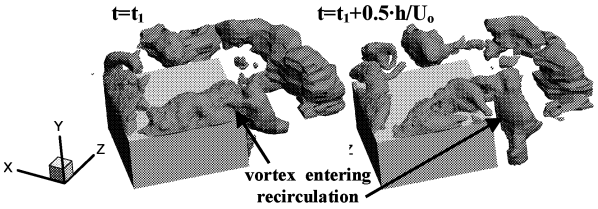

Figure 2. Snapshots of iso-pressure surfaces (C_p=1.67) portraying conical vortex development and shedding.

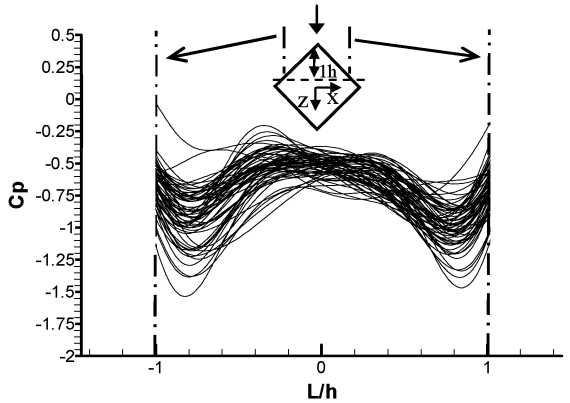

Figure 3. Instantaneous pressure coefficient distributions at a distance of 1h from the leading corner of the cubicle roof for a period of 10(h/U_o)

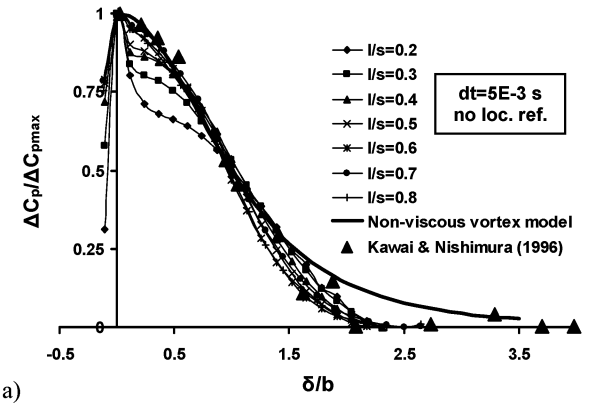

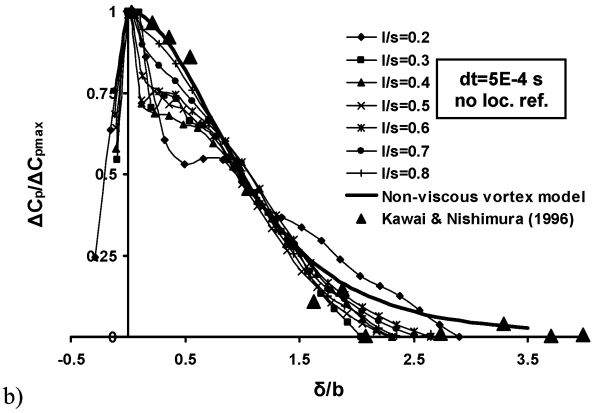

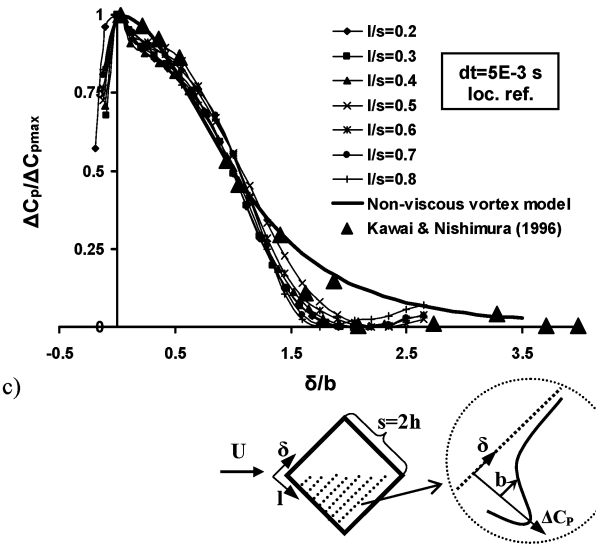

Figure 4. Similarity of mean pressure coefficient profiles in the direction normal to the side of the roof. a) dt=5.E-3, without local grid refinement, b) dt=5E-4, without local grid refinement, c) dt=5E-3, with local grid refinement.

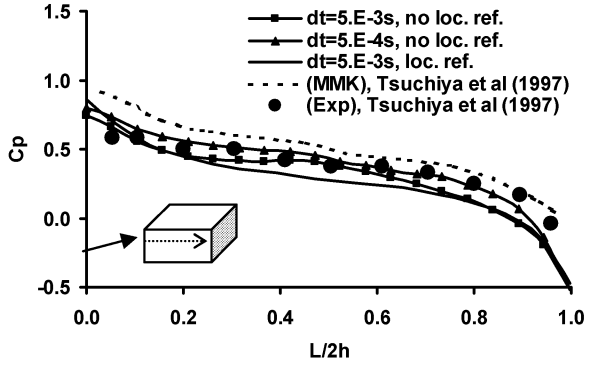

Figure 5. Horizontal profile of the mean pressure coefficient along the leading face of the cubicle 0.66h from the bottom.

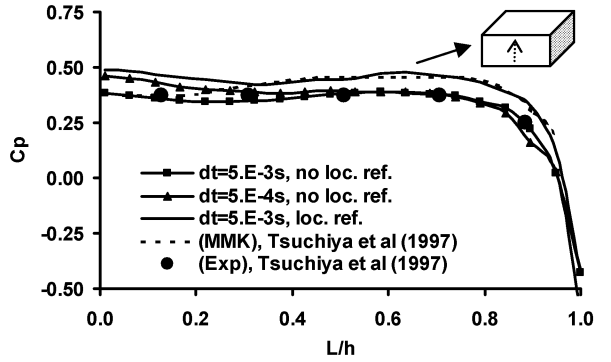

Figure 6 Vertical profiles of the mean pressure coefficient in the middle of the leading face of the cubicle.

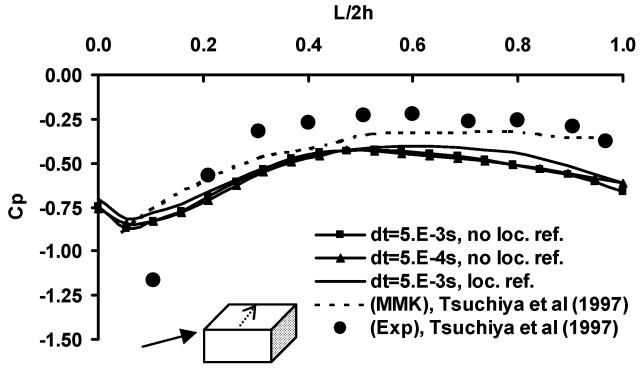

Figure 7 Mean pressure coefficient along the top of the cubicle in a direction perpendicular to the side edge.

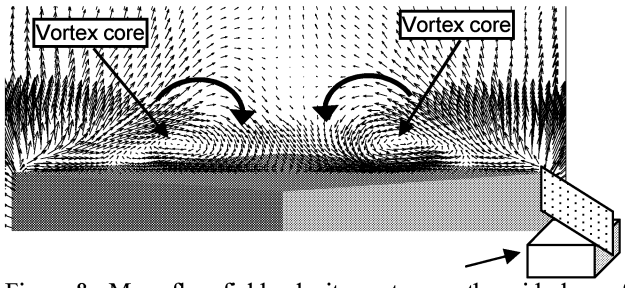

Figure 8. Mean flow field velocity vectors on the mid plane of the cubicle normal to the flow direction (z=0). Cores of conical vortices are indicated.

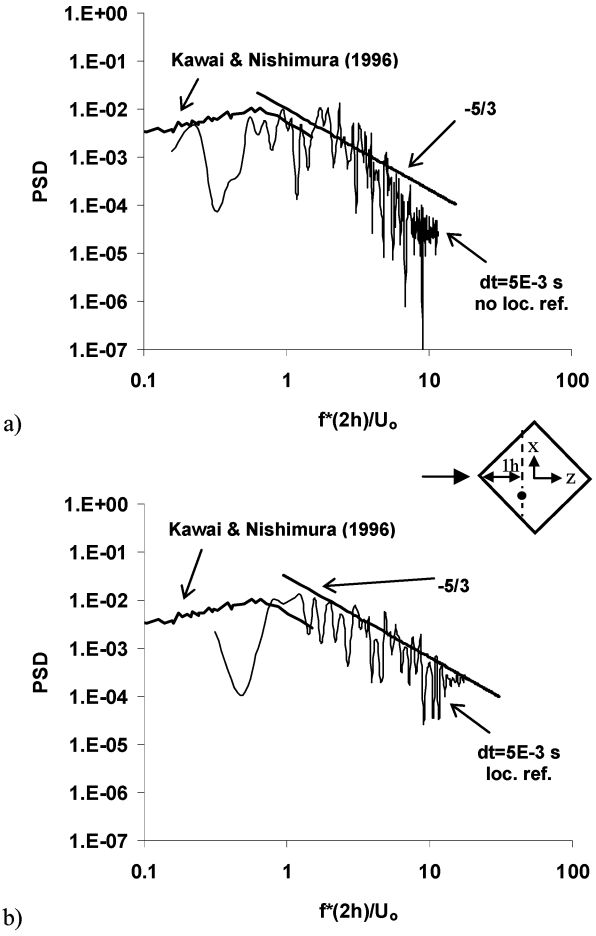

Figure 9. Power spectral density of the fluctuation pressure coefficient at the roof top a) calculated without local grid refinement, b) with local grid refinement.